Theoretical analysis of various climatic parameter effects on performance of a basin solar still

Masoud Afrand*, Arash Karimipour

Department of Mechanical Engineering, Najafabad Branch, Islamic Azad University, Najafabad, Iran

Abstract

A numerical simulation of a basin solar still under various climatic parameters was performed. The proposed system was modeled using the mass and energy balance equations of different parts of the solar still. The resulting system of nonlinear algebraic equations was solved numerically and the effect of various parameters, such as wind speed, air temperature and solar radiation on the amount of distilled water produced was described. The results showed that the ambient temperature and wind speed had no significant effect on the amount of distilled water produced, while the amount of solar radiation exerted a direct effect on the amount of distilled water produced and performance of the system.

Keywords: Theoretical analysis, Basin solar still, Climatic parameters, Efficiency, Desalination

1. Introduction

Development of renewable energies such as solar energy has attracted many researchers' attention in recent years [1–4]. Researchers reported that wherever water is available, solar desalination has been one of the best ways to produce potable water. However, the rapid increase in prices of different fossil fuels and the availability of solar energy in recent years, even in remote areas of the world, has increased the attractiveness of solar energy. Therefore, researchers have carried out studies in the context of improving the use of solar energy. For example, some researchers proposed new working fluids for solar systems [5–9].

Basin solar stills could be used as a useful technology for producing distilled water from salt water [10, 11].This process occurs primarily based on water surface evaporation and condensation of water vapor. Many studies have been conducted in the field of basin solar still types, examining various methods of optimizing the desalination process and functional efficiency of various pieces of apparatus [12, 13].

Encountering the problem of storage in distillation equipment, i.e. the accumulation of salt, Minassian et al. [14] evaluated the possibility of increasing the production rate of a basin solar still with a common pond model using a cylindrical parabolic reflector. They found that the production rate of the solar distillation equipment with a common pond model was increased through the use of a cylindrical parabolic reflector made of stainless steel. The results showed that the production rate of the new solar distillation apparatus was 35–25% higher than the rate of production of solar distillation equipment with a common pond model. Kumar et al. [15] showed numerically the annual performance of solar distillation equipment for the climatic conditions of Delhi. They provided analytical expressions for the temperature of the water, the glass cover, efficiency based on design, and climatic parameters. It was observed that for the given parameters, the annual production was optimal when the slope of the aggregate was 20° and the slope of the glass cover of distillation equipment was 15°. Ayav et al. [16] performed research in the IZTECH database, experimentally and numerically. Comparison between the two studies suggested good agreement between the experimental results and the results of theoretical calculations. Moreover, their study showed that the efficiency of the system achieves up to 45% in March, producing up to 3.5 l/m² day of distilled water. Radwan et al. [17] carried out a comparison between the experimental results and those of theoretical calculations for a basin solar still in Egypt. They derived the amount of production of distilled water from a system with specific dimensions for 4 months and showed that the mean production of distilled water in August was higher than the amount produced in June and July. Rajan et al. [18] investigated the use of a multi basin solar still to increase productivity. They integrated the multi basin still with a biomass heat source. Their system increased the water temperature in the sword and increased productivity
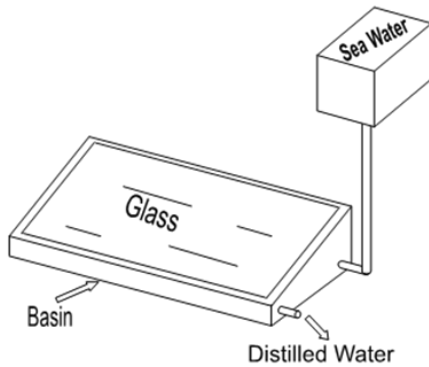

Figure 1: Schematic illustration of a basin solar still

in the blade. Asbik et al. [19] presented an exergy analysis of a passive solar still combined with a heat storage system. They used paraffin wax as phase change material (PCM) to store/retrieve energy. They determined the magnitude of exergy losses during the heat storage/retrieve period. They found that latent heat storage enhanced water productivity and reduced exergy efficiency. Srithar et al. [20] experimentally tested a stand-alone triple basin solar desalination system. Their results revealed that a triple basin glass solar still (TBSS) with charcoal and TBSS with river sand enhance the distillate by 34.2 and 25.6% more than conventional TBSS distillates. They also found that the presence of a concentrator increased the lower basin water temperature by up to 85°C. They achieved a maximum distillate yield of 16.94 kg/m^{2}day for TBSS with a concentrator, cover cooling and charcoal in fins.

A review of previous works revealed that basin solar stills have been experimentally and theoretically investigated in many studies in several countries. However, basin solar stills are less studied in Iran compared to other countries. Moreover, some assumptions have been considered that do not often happen in reality. Hence, in this paper, efforts are made to simulate an actual basin solar still with minimal assumptions. To achieve this purpose, a thermal model for estimating the efficiency of a basin solar still is introduced, using the mass and energy balance equations of different parts of the solar still. Then, the influence of different climatic disturbances on system performance, specifically wind speed, ambient temperature and hourly solar irradiation is investigated.

2. Statement of the problem

In this paper, a basin solar still (Fig. 1) is numerically simulated. The main components of a solar desalination unit are as follows:

- Pond for storing a sufficient amount of salt water

- Transparent cover (glass or plastic) to allow solar radiation to pass with minimum loss of energy

- Channels for collecting distilled water

The water pond is 10 cm deep. The temperature of the surface water is considered T_i. The transparent cover, which plays an important role in energy absorption, is exposed to solar radiation. This surface is in contact with air from the outside. The temperature of the glass cover is considered T_g. The bottom of the pond, which is usually a black plate, is responsible for absorbing energy. The bottom of pond temperature is also considered T_b. The inside air of the desalination chamber is constantly saturated and is considered temperature T_r.

In a simple basin solar still, the whole process is based on surface evaporation. The water is heated by the radiation emitted from the sun. The water is then heated and evaporates and rises to the glass cover because of the density difference. The temperature of the coating is lower than the internal air temperature of the still. Therefore, the saturated moist air in the still condenses on reaching the glass cover, the condensed heat warms the glass coating and heat is exchanged with the surroundings and the air in the still by convection and radiation. Liquid droplets flow down and are gathered in a channel at the southern end of the glass cover of the still and, then, are collected in a reservoir outside the still. The efficiency of the basin solar still equals the rate of evaporated water divided by the amount of radiation in the surface unit of thepond on a given day. The performance of a basin solar still can be described by writing the energy and mass balance equations for various components of the still.

3. The equations and computational model

The general details of the computational model are based on the laws of mass and energy conservation in every part of the desalination unit. The main assumptions in establishing a physical model are defined as follows:

- The whole system is in a steady state. This means that at one hour intervals, the system is assumed to be stable.

- The heat loss by radiation from the walls of the chamber (except the glass cover) is negligible.

- Due to distillation, the temperature of the walls is equal to the water temperature, which is the average of interface temperature and the bottom temperature.

- Some thermo-physical properties of fluid variable with temperature including thermal conductivity, density, specific heat and convective heat transfer coefficient (for ambient air) can be considered constant.

- The desalination unit and its parts are considered as the control volume, and the resistance to heat transfer of the thermal conductivity of glass is neglected.

Firstly, mass and energy balance equations should be considered for the entire desalination unit (Eq. 1).
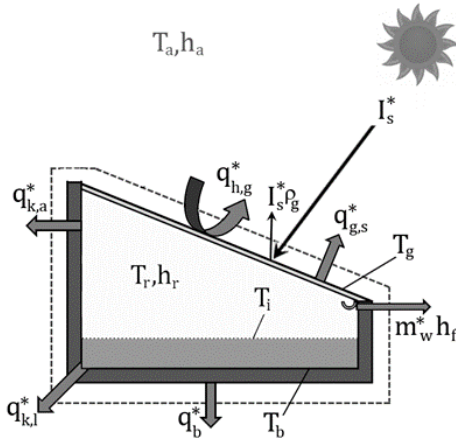
Figure 2: Energy balance for the whole of the solar still

Figure 3: Energy balance for the glass cover

Energy balance in Fig. 2 shows that the energy of condensation and heat is transferred from the atmosphere to the distillation desalination.

$$I_s^* A_g = I_s^* \rho_g A_g + q_{g,s}^* A_g + q_{h,g}^* A_g \\ + q_{k,a}^* A_{k,a} + q_{k,l}^* A_{k,l} + q_b^* A_b + m_w^* h_f \tag{1}$$

I_s^* is the intensity of solar radiation and ρ_g is the reflectivity of the glass cover for visible light.

With regard to the heat transfer from the atmosphere by convection, the following is obtained:

$$q_{h,g}^* = h_w \left(T_g - T_a \right) \tag{2}$$

where T_g and T_a are the glass temperature and ambient temperature, respectively. h_w is the convective heat transfer coefficient, and it is given by Eq. 3 [16]:

$$h_w = 5.7 + 3.8w \tag{3}$$

In this equation, the convection coefficient depends on the wind speed.

Radiant heat transfer from the glass cover to atmosphere air is:

$$q_{g,s}^* = \varepsilon_g \sigma \left[\left(T_g \right)^4 - \left(T_{sky} \right)^4 \right] \tag{4}$$

where, σ is the Boltzmann constant (5.667×10^{-8} W / m^{2}K^4) and σ is glass emissivity for infrared radiation ($\varepsilon_g = 0.88$). Sky temperature (T_{sky}) can be calculated from the Eq. 5 [21]:

$$T_{sky} = 0.0552 \, T_a^{1.5} \tag{5}$$

where T_a and T_{sky} are in terms of Kelvin.

Conductive heat transfer from the bottom to the atmosphere can be formulated as follows:

$$q_b^* = \frac{(T_b - T_a)}{\frac{1}{h_{in}} + \sum \frac{\delta_i}{\lambda_i} + \frac{1}{h_w}} \tag{6}$$

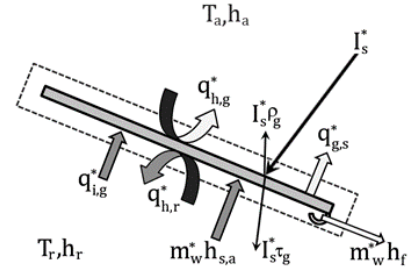where h_{in} is assumed an infinity for liquid water.

Considering the heat transfer by conduction from the peripheral desalination humid air into the atmosphere, we have:

$$q_{k,a}^* = \frac{(T_r - T_a)}{\frac{1}{h_r} + \sum \frac{\delta_i}{\lambda_i} + \frac{1}{h_w}} \tag{7}$$

where h_r is calculated by Eq. 12.
Heat transfer from the liquid to the atmosphere is:

$$q_{k,l}^* = \frac{[(T_i + T_b)/2 - T_a]}{\frac{1}{h_{in}} + \sum \frac{\delta_i}{\lambda_i} + \frac{1}{h_w}} \tag{8}$$

where h_{in} is assumed an infinity for liquid water. h_f is enthalpy of the saturated water at T_g, and m_w^* is the mass flow rate of condensed water.

Using Fig. 3, the energy balance equation for the glass cover is as follows:

$$I_s^* A_g + q_{i,g}^* A_g \cos\beta + q_{h,r}^* A_g + m_w^* h_{s,a} = \\ I_s^* \rho_g A_g + I_s^* \tau_g A_g + q_{g,s}^* A_g + q_{h,g}^* A_g + m_w^* h_f \tag{9}$$

β is the angle of the glass cover, $q_{i,g}^*$ is radiation heat flux from the surface of the water in the glass, $q_{h,r}^*$ is convective heat flux from the water to the glass cover, $h_{s,a}$ is enthalpy of saturation water at T_r, and τ_g is glass transmission coefficient for visible light radiation.

Radiation heat transfer from the water to the glass cover is as follows [16]:

$$q_{i,g}^* = \frac{\left(T_i^4 - T_g^4 \right) + \left(\frac{1-\varepsilon_g}{\varepsilon_g} \right) \times \tau_g' \times T_i^4}{\left(\frac{1}{\varepsilon_g \sigma} + \frac{1}{\varepsilon_w \sigma} - \frac{1}{\sigma} + \frac{1-\varepsilon_w-\varepsilon_g}{\varepsilon_w \varepsilon_g \sigma} \tau_g' \right)} \tag{10}$$

ε_g is glass emissivity and τ_g' is glass transmission coefficient for infrared radiation.

Convective heat transfer from the water to the glass cover is:

$$q_{h,r}^* = h_r \left(T_r - T_g \right) \tag{11}$$

Convection heat transfer coefficient (h_r) is presented as follows [22]:

$$h_r = 0.884 \left[\left(T_i - T_g \right) + \frac{P_i - P_g}{268900 - P_i} T_i \right]^{1/3} \tag{12}$$
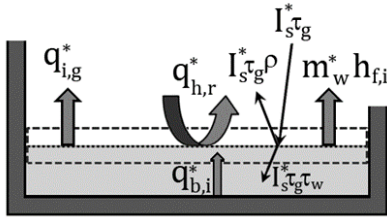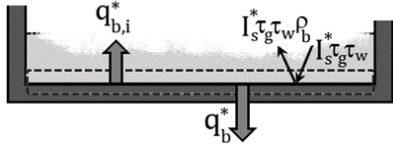
Figure 4: Energy balance for the interface

Figure 5: Energy balance for the black plate

In Eq. 12, P_i and P_g are steam pressure at T_i and T_g, respectively. These pressures have been obtained from Eq. 13 [23]:

$$P_{partial} = \exp\left[25.317 - \frac{5144}{T}\right] \quad (13)$$

Referring to Fig. 4, energy balance for the interface can be written as follows:

$$I_s^* \tau_g A_g + q_{b,i}^* A_b = I_s^* \tau_g \rho_w A_b + I_s^* \tau_g \tau_w A_b \\ + q_{i,g}^* A_b + q_{h,r}^* A_b + m_w^* h_{f,i} \quad (14)$$

where $q_{i,g}^*$ is radiation heat flux from the surface of the water in the glass from Eq. 10, τ_w is transmission coefficient of water, r_w is reflection coefficient of water, $h_{f,i}$ is enthalpy of water at T_i and m_w^* is evaporation rate of moist air.
Conductive heat transfer from the floor to the interface is:

$$q_{b,i} = \frac{\lambda_w}{\delta_w} (T_b - T_i) \quad (15)$$

The convection of seawater interface to the glass cover is:

$$q_{h,r} = h_r (T_i - T_r) \quad (16)$$

The energy balance equation for the black plate according to Fig. 5 can be written as follows:

$$I_s^* \tau_g \tau_w A_b - I_s^* \tau_g \tau_w \rho_b A_b = q_{b,i}^* A_b + q_b^* A_b \quad (17)$$

where, ρ_b is reflection coefficient of the black plate.
As noted in the above equations, m_w is the mass flow rate of condensed water, which is equal to the mass flow rate of the evaporated water mass. This mass flow rate can be determined by Eq. 18 [24].

$$m_w^* = h_{M,h} \frac{1}{RT} (P_i - P_r) A_b \quad (18)$$

Table 1: Constant values used in calculations

Parameter	Description	Value
ε_g	Emissivity of glass	0.880
ε_w	Emissivity of water	0.900
ρ_g	Reflectivity of glass cover	0.050
ρ_w	Reflectivity of water	0.001
τ_g	Glass transmittance for visible light	0.824
τ_g	Transmittance of water	0.999
τ_g'	Transmittance of glass for infrared radiation	0.045
		0.045

T denotes the internal saturated air temperature in Kelvin, and R indicates the universal gas constant. Moreover, P_i and P_r are the water vapor partial pressures at T_i and T_r, respectively.
In Eq. 18, $h_{M,h}$ is the mass transfer coefficient for the semi-permeable plane and can be expressed as [16]:

$$h_{M,h} = h_M \frac{P}{P_i - P_r} \ln\left(\frac{P - P_r}{P - P_i}\right) \quad (19)$$

where h_M is the mass transfer coefficient for the non-permeable plane in (m/s) [16] and P is the internal air pressure of the still.
The hourly efficiency of the basin solar still can be calculated by the following [16]:

$$\eta = \frac{m_{w,t}^* \times 2501.3}{I_{s,t} \times A_g} \times 100\% \quad (20)$$

where m^* is the total condensed water in one hour, 2501.3 ml is the vaporization latent heat of water, $I_{s,t}$ is the total solar radiation per day and A_g is the area of the glass cover.
The constant values used in calculations are presented in Table 1.

4. The solution of equations

According to the obtained system of nonlinear algebraic equations, nonlinear equations with four unknowns T_b, T_i, T_r and T_g were obtained. To solve this system, a computer program was written based on the energy balance equations to obtain the temperature of the glass cover, internal moist air, bottom and interface. The values of these temperatures could help us in the theoretical study of the amount of evaporated water in solar radiation with ambient temperature. In this program, the Newton-Raphson algorithm was used to solve the system of nonlinear algebraic equations.

5. Results and Discussion

First, to assure the accuracy of the numerical results for the basin solar still, a comparison was made between the results of the present work and those of Ayav et al. [16] on 28th April 2003. Three rows of comparative numbers are provided in Table 2. Despite the unavailability of some input parameters [16], the results obtained in the present work show

Table 2: Comparison of the results of the present work with the research conducted by Ayav et al. [16] on 28th April 2003

	Time	Tbottom	Tmoistair	Tinterface	Tglass
Ayav et al. work [16]					
	10--11	62.26	45.01	53.47	25.97
	11--12	73.91	58.19	64.12	28.65
	12--13	89.06	76.38	79.12	35.98
Present work	10--11	64.03	46.18	54.45	26.34
	11--12	76.41	59.83	64.61	28.97
	12--13	91.60	78.82	80.12	36.35

Figure 7: Hourly variation of temperature values in the basin solar still (Wind speed: 2 m/s, ambient temperature: 30°C)

Figure 6: Hourly variation of absorption of solar radiation on 6th July [25]

Figure 8: Hourly variation of distilled water values in the basin solar still (Wind speed: 2 m/s, ambient temperature: 30°C)

good agreement. It seems that the proposed model in this paper is suitable for the analysis of different parameters.

Table 2. Comparison of the results of the present work with the research conducted by Ayav et al. [16] on 28th April 2003

An initial investment is required to build desalination plants. Another important parameter is the adaptation of desalination to different climatic conditions. Therefore, in this paper, the effect of parameters such as wind speed, ambient temperature and solar radiation on the amount of distilled water is investigated. This study was conducted for the city of Chabahar on 6 July. The solar desalination unit has an inclined glass at an angle equal to the latitude of Chabahar (25 degrees to the south) where the maximum amount of radiation is absorbed [9].

Based on the extracted reference values [25], the hourly variation of absorption of solar radiation on 6th July for the city of Chabahar is shown in Fig. 6.

In Fig. 7, the hourly variation temperature of different parts of the desalination unit is displayed. It can be seen that the hourly variation in temperature is similar to the hourly variation of solar radiation absorption. Moreover, it is observed that the maximum and minimum temperature occur at the bo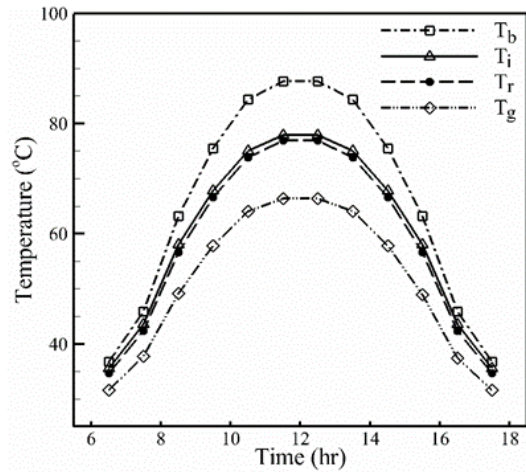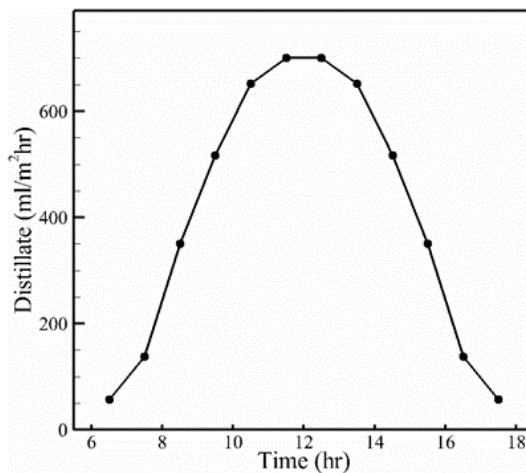ttom of the pond and glass cover, respectively. In addition, it can be found that interface temperature and saturation temperature differences are small due to the evaporation process. At noon, when solar radiation is higher, the temperature difference between the bottom, the glass cover and the interface increases significantly.

Fig. 8 shows the hourly variation of distilled water values in the basin solar still. By comparing this figure with Fig. 6, it can be seen that the rate of distilled water produced is directly related to the amount of solar radiation. In addition, this figure reveals that the rate of distillation increases to 700 ml/hr per square meter of glass cover at noon. As seen in Fig. 7, the temperature difference between the glass cover and the interface temperature increases at noon. Thus, according to Eq. 12, the convective heat transfer coefficient increases, and consequently the rate of evaporation and condensation goes up.
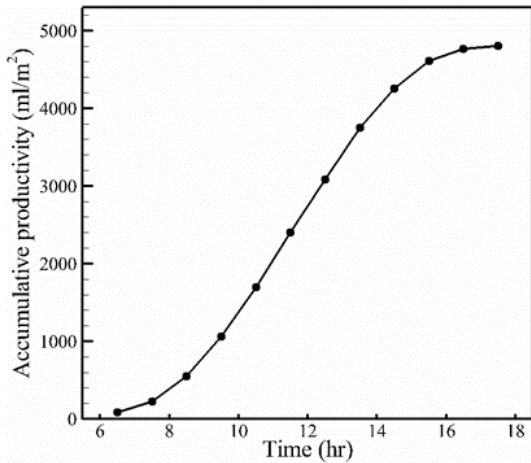
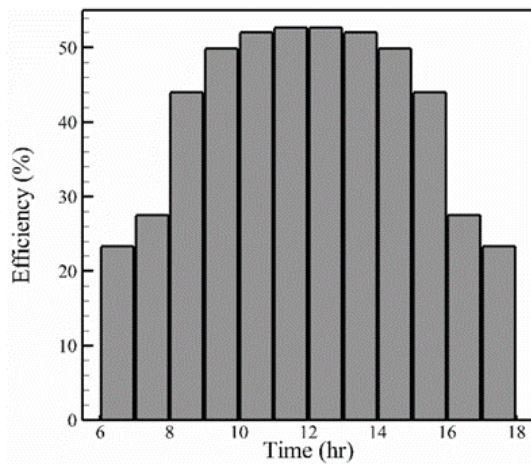Figure 9: Hourly variation of accumulative productivity (wind speed: 2 m/s, ambient temperature: 30°C)

Figure 10: Hourly variation of efficiency (wind speed: 2 m/s, ambient temperature: 30°C)

Hourly variation of accumulative productivity is shown in Fig. 9. The distilled water produced is 4.806 lit/m^2 from 6:30 to 17:30. As can be seen, the production rate begins slowly in the morning but increases at noon.

The hourly variation of efficiency is presented in Fig. 10. It can be observed that the efficiency increases to 50% at noon. From this figure, it is clear that there is a direct relationship between efficiency and the amount of solar radiation.

Effect of wind speed on the amount of distilled water produced is reported in Table 3. The ambient temperature is considered constant (30°C). As can be seen, the wind speed has little influence on the amount of distilled water produced (maximum 2% for wind speed of 10 m/s). However, it seems that when solar radiation is high, wind speed increases the production of distilled water.

The effect of ambient temperature on the amount of distilled water produced is presented in Table 4. The wind speed is considered constant (2 m/s). It can be seen that for a 20 degree rise in ambient temperature in the morning

Table 3: Effect of wind speed on the production of distilled water

Time	$V = 0$ ml/m^2	$V = 10$ m/s ml/m^2	Difference %
7–8	138.41	137.85	-0.40
8–9	349.92	349.39	-0.15
9–10	515.64	521.80	1.19
10–11	643.57	659.49	2.47
11–12	694.03	721.06	3.89
Total	2341.57	2389.59	2.05

Table 4: Effect of ambient temperature on the production of distilled water

Time	$T_{amb} = 20°C$ ml/m^2	$T_{amb} = 40°C$ ml/m^2	Difference %
7–8	131.56	140.35	6.68
8–9	343.37	351.2	2.28
9–10	514.07	517.72	0.71
10–11	647.42	647.26	-0.02
11–12	700.12	698.52	-0.23
Total	2336.54	2355.05	0.79

(when solar radiation is low), the amount of distilled water produced increases 6.68%. At noon (when solar radiation is high), the amount of distilled water produced does not change if the ambient temperature is varied.

6. Conclusion

Analysis of the effects of selected climatic parameters on a basin solar still was carried out for the city of Chabahar (Iran) on 6th July and the results are as follows:

1. Rate of distillation increases to 700 ml/hr per square meter of glass cover at noon on 6th July.
2. The distilled water produced is 4.806 lit/m^2 from 6:30 to 16:30.
3. Efficiency increases to 50% at noon, and there is a direct relationship between efficiency and the amount of solar radiation.
4. Wind speed does not much influence on the amount of distilled water produced.
5. For a 20-degree rise in ambient temperature in the morning (solar radiation is low), the amount of distilled water produced increases 6.68%.
6. At noon (solar radiation is high), the ambient temperature has little influence on the amount of distilled water produced.

References

[1] P. Krawczyk, K. Badyda, Modelling of thermal and flow processes in a solar waste-water sludge dryer with supplementary heat supply from external sources., Journal of Power Technologies 91 (1) (2011) 37.

[2] R. D. Tapakis, A. G. Charalambides, Performance evaluation of a photovoltaic park in cyprus using irradiance sensors, Journal of Power Technologies 94 (4) (2014) 296.

[3] A. Wyrwa, A. Szurlej, L. Gawlik, W. Suwala, Energy scenarios for poland-a comparison of primes and times-pl modeling results, Journal of Power Technologies 95 (5) (2015) 100.

[4] F. Zebiri, A. Kessal, L. Rahmani, A. Chebabhi, Analysis and design of photovoltaic pumping system based on nonlinear speed controller, Journal of Power Technologies 96 (1) (2016) 40.

[5] M. Afrand, D. Toghraie, B. Ruhani, Effects of temperature and nanoparticles concentration on rheological behavior of fe 3 o 4–ag/eg hybrid nanofluid: an experimental study, Experimental Thermal and Fluid Science 77 (2016) 38–44.

[6] M. Baratpour, A. Karimipour, M. Afrand, S. Wongwises, Effects of temperature and concentration on the viscosity of nanofluids made of single-wall carbon nanotubes in ethylene glycol, International Communications in Heat and Mass Transfer 74 (2016) 108–113.

[7] H. Eshgarf, M. Afrand, An experimental study on rheological behavior of non-newtonian hybrid nano-coolant for application in cooling and heating systems, Experimental Thermal and Fluid Science 76 (2016) 221–227.

[8] M. Soltanimehr, M. Afrand, Thermal conductivity enhancement of cooh-functionalized mwcnts/ethylene glycol–water nanofluid for application in heating and cooling systems, Applied Thermal Engineering 105 (2016) 716–723.

[9] D. Toghraie, V. A. Chaharsoghi, M. Afrand, Measurement of thermal conductivity of zno–tio2/eg hybrid nanofluid, Journal of Thermal Analysis and Calorimetry 125 (1) (2016) 527–535.

[10] A. Kaushal, et al., Solar stills: A review, Renewable and Sustainable Energy Reviews 14 (1) (2010) 446–453.

[11] M. S. S. Abujazar, S. Fatihah, A. Rakmi, M. Shahrom, The effects of design parameters on productivity performance of a solar still for seawater desalination: A review, Desalination 385 (2016) 178–193.

[12] T. Rajaseenivasan, K. Kalidasa Murugavel, Performance and exergy analysis of a double-basin solar still with different materials in basin, Desalination and Water Treatment 55 (7) (2015) 1786–1794.

[13] H. N. Panchal, P. K. Shah, Enhancement of upper basin distillate output by attachment of vacuum tubes with double-basin solar still, Desalination and Water Treatment 55 (3) (2015) 587–595.

[14] A. Minasian, A. Al-Karaghouli, S. Habeeb, Utilization of a cylindrical parabolic reflector for desalination of saline water, Energy conversion and management 38 (7) (1997) 701–704.

[15] S. Kumar, G. Tiwari, H. Singh, Annual performance of an active solar distillation system, Desalination 127 (1) (2000) 79–88.

[16] P. İ. Ayav, G. Atagündüz, Theoretical and experimental investigations on solar distillation of iztech campus area seawater, Desalination 208 (1-3) (2007) 169–180.

[17] S. Radwan, A. Hassanain, M. Abu-Zeid, et al., Single slope solar still for sea water distillation., World Applied Sciences Journal 7 (4) (2009) 485–497.

[18] A. S. Rajan, K. Raja, P. Marimuthu, Multi basin desalination using biomass heat source and analytical validation using rsm, Energy Conversion and Management 87 (2014) 359–366.

[19] M. Asbik, O. Ansari, A. Bah, N. Zari, A. Mimet, H. El-Ghetany, Exergy analysis of solar desalination still combined with heat storage system using phase change material (pcm), Desalination 381 (2016) 26–37.

[20] K. Srithar, T. Rajaseenivasan, N. Karthik, M. Periyannan, M. Gowtham, Stand alone triple basin solar desalination system with cover cooling and parabolic dish concentrator, Renewable Energy 90 (2016) 157–165.

[21] W. C. Swinbank, Long-wave radiation from clear skies, Quarterly Journal of the Royal Meteorological Society 89 (381) (1963) 339–348.

[22] R. Dunkle, Solar water distillation: the roof type still and the multiple effect diffusor, Int. Dev. in Heat Transfer;().

[23] J. Fernández, N. Chargoy, Multi-stage, indirectly heated solar still, Solar energy 44 (4) (1990) 215–223.

[24] Grundgesetze der Waermeubertrgung, Springer-Verlag, 1963, Grigull U.

[25] M. Afrand, A. Behzadmehr, A. Karimipour, A numerical simulation of solar distillation for installation in chabahar-iran, World Academy of Science, Engineering and Technology 47 (2010) 469–474.

Nomenclature

A_g	glass cover surface, m^2
T_g	Temperature of glass cover, °C or K
T_r	temperature of saturated air, °C or K
T_{sky}	Temperature of sky, °C or K
h_M	mass transfer coefficient for non-permeable plane, m/s
I_s^*	solar radiation intensity, W/m^2
I_{st}	total solar radiation in one hour, kJ/m^{2}hr
m_w^*	the mass flow rate of condensed water, kg/s
$m_{w,t}$	total condensed water in one hour, kg/m^{2}s
P	inside air pressure of still, N/m^2
P_i	water vapor partial pressure at T_i, N/m^2
A_b	bottom area covered by the seawater, m^2
P_g	water vapor partial pressure at T_g, N/m^2
P_r	water vapor partial pressure at T_r, N/m^2
q^*	heat transfer per unit area, W/m^2
T_a	temperature of ambient air, °C or K
T_b	temperature of bottom, °C or K
T_a	temperature of interface, °C or K
w	width of basin and reflector, m
β	angle of glass cover
$A_{k,l}$	circumferential area of solar still covered by saline water, m^2
$A_{k,a}$	circumferential area of solar still covered by inside saturated air, m^2
h_r	convective heat transfer coefficient of inside saturated air, W/m^{2}K
h_w	convective heat transfer coefficient of ambient air, W/m^{2}K
h_{in}	convective heat transfer coefficient of saline water, W/m^{2}K
$h_{s,a}$	enthalpy of saturated water at T_r, kJ/kg
h_f	enthalpy of saturated water at T_g, kJ/kg

Greek letters

δ	thickness, m

τ_w	transmittance of water
ε_g	emissivity of the glass
ε_w	emissivity of water
η	hourly efficiency
λ	thermal conductivity, W/mK
ρ_w	reflectivity of water
ρ_g	reflectivity of glass
ρ_b	reflectivity of black basin bottom
σ	Stefan–Boltzmann constant, $=5.67 \times 10^{-8}$ W/m^2 K^4
τ_g	glass transmittance for visible light
τ_g'	transmittance of glass for infrared radiation